Key Intermediate Species Reveal the Copper(II)-Exchange Pathway in Biorelevant ATCUN/NTS Complexes

Kotuniak, Radosław; Strampraad, Marc J.F.; Bossak-Ahmad, Karolina; Wawrzyniak, Urszula E.; Ufnalska, Iwona; Hagedoorn, Peter Leon; Bal, Wojciech

DOI
10.1002/anie.202004264

Publication date
2020

Document Version
Final published version

Published in
Angewandte Chemie - International Edition

Bioinorganic Chemistry Hot Paper

How to cite:
International Edition: doi.org/10.1002/anie.202004264
German Edition: doi.org/10.1002/ange.202004264

Key Intermediate Species Reveal the Copper(II)-Exchange Pathway in Biorelevant ATCUN/NTS Complexes

*Radosław Kotuniak, Marc J. F. Strampraad, Karolina Bossak-Ahmad, Urszula E. Wawrzyniak, Iwona Ufnalska, Peter-Leon Hagedoorn, and Wojciech Bal**

Abstract: *The amino-terminal copper and nickel/N-terminal site (ATCUN/NTS) present in proteins and bioactive peptides exhibits high affinity towards Cu^{II} ions and have been implicated in human copper physiology. Little is known, however, about the rate and exact mechanism of formation of such complexes. We used the stopped-flow and microsecond freeze-hyperquenching (MHQ) techniques supported by steady-state spectroscopic and electrochemical data to demonstrate the formation of partially coordinated intermediate Cu^{II} complexes formed by glycyl–glycyl–histidine (GGH) peptide, the simplest ATCUN/NTS model. One of these novel intermediates, characterized by two-nitrogen coordination, $t_{1/2} \approx 100$ ms at pH 6.0 and the ability to maintain the Cu^{II}/Cu^{I} redox pair is the best candidate for the long-sought reactive species in extracellular copper transport.*

Alterations of exchangeable Cu^{II} in blood have been implicated in a number of severe human diseases including diabetes, cancer, and Alzheimer's disease.[1] Some human proteins involved in these processes contain the metal-binding ATCUN/NTS motifs (amino-terminal copper and nickel/N-terminal site), tripeptide sequences containing a free amine at the N-terminus, any amino acid residue in position 2, and a His residue in position 3. In addition to Cu^{II} ions, Ni^{II}, Pd^{II}, and Au^{III} can bind to ATCUN/NTS in a specific manner, forming square planar four-nitrogen (4N) complexes with the terminal amine, two intervening peptide bond nitrogen atoms and the imidazole N3 nitrogen coordinated. These structures were documented by X-ray crystallography,[2,3] EXAFS,[3–5] NMR,[6] and numerous spectroscopic studies, as reviewed recently.[7] The Asp–Ala–His motif in human serum albumin (HSA) and analogous motifs in other albumins transport Cu^{II} in blood serum,[8] and are thought to deliver it to another ATCUN/NTS motif present in the extracellular domain of Ctr1 cellular copper transporters of many species (Met–Asp–His in human Ctr1, hCtr1).[9] Molecular aspects of this process remain to be elucidated. A direct non-redox, but rather sluggish transfer ($t_{1/2} \approx 16$ min) was recently demonstrated in vitro using HSA and a 14-peptide model of hCtr1 N-terminus.[5] On the other hand, the rates of such Cu^{II} transfers from 4N complexes to stronger ligands could be accelerated by weakly chelating agents, which did not participate significantly in the Cu^{II} equilibrium, for example, the Cu^{II} transfer from the $Cu^{II}A\beta_{4\text{-}16}$ complex to EDTA, accelerated by glutamate addition.[10,11] The 4N Cu^{II} complexes cannot be reduced electrochemically to the corresponding Cu^{I} species. They can be oxidized to Cu^{III} only at high potentials around 1 V,[3,11,12] but in an apparent contradiction with this fact, these 4N complexes were demonstrated recently to generate reactive oxygen species (ROS) under physiologically relevant conditions via an unidentified Cu^{I} species.[13] These pieces of evidence, taken together, suggest the existence of distinct intermediate complex(es) responsible for kinetic and redox properties of nominally 4N ATCUN/NTS Cu^{II} complexes.

Gly–Gly–His (GGH) is the simplest ATCUN/NTS peptide, also used as Cu^{II} chelator in practical applications, for example, enhancing the efficacy of antimicrobial peptides,[14] and copper sensing.[15] Herein, we present the stopped-flow and microsecond timescale freeze hyperquenching (MHQ)[16] data combined with UV/Visible and EPR spectroscopic and electrochemical evidence for transient Cu^{II}/GGH complexes that have been unnoticed before. These results explain the reactivity of ATCUN/NTS complexes and their contribution to biological Cu^{II} transport.

We first studied the reaction of GGH with $CuCl_2$ at pH 6.0 using a stopped-flow system coupled with a diode-array detector working in the 750–300 nm range. This pH value was chosen to assure complete formation of the 4N complex, limit the formation of poorly soluble $Cu(OH)_2$, and allowed us to use a buffer that does not coordinate Cu^{II} ions.[17] All these needs were fulfilled by using 2-(*N*-morpholino)ethanesulfonic acid (MES), with a pK_a of 6.15.[18] The obtained spectra (Figure 1) show the increase in time of the *d–d* band, λ_{max} (ε) = 525 nm ($102\ M^{-1}cm^{-1}$), characteristic of the 4N complex.[7,19–23] This effect is coupled by an isosbestic point at 620 nm to the depletion of the initial band, λ_{max} (ε) = 705 nm (48). The latter band was present at its maximum intensity already in the first recorded spectrum after circa 2 ms of the reaction initiation. The formation of the 525 nm band, which

[*] R. Kotuniak, K. Bossak-Ahmad, Prof. W. Bal
Department of Biophysics, Institute of Biochemistry and Biophysics
Polish Academy of Sciences
Pawińskiego 5a, 02-106 Warsaw (Poland)
E-mail: wbal@ibb.waw.pl
M. J. F. Strampraad, Dr. P.-L. Hagedoorn
Department of Biotechnology, Delft University of Technology
Van der Maasweg 9, 2629 HZ Delft (The Netherlands)
Dr. U. E. Wawrzyniak, I. Ufnalska
Chair of Medical Biotechnology, Faculty of Chemistry, Warsaw
University of Technology, Noakowskiego 3, 00-664 Warsaw (Poland)
Supporting information and the ORCID identification number(s) for the author(s) of this article can be found under:
https://doi.org/10.1002/anie.202004264.

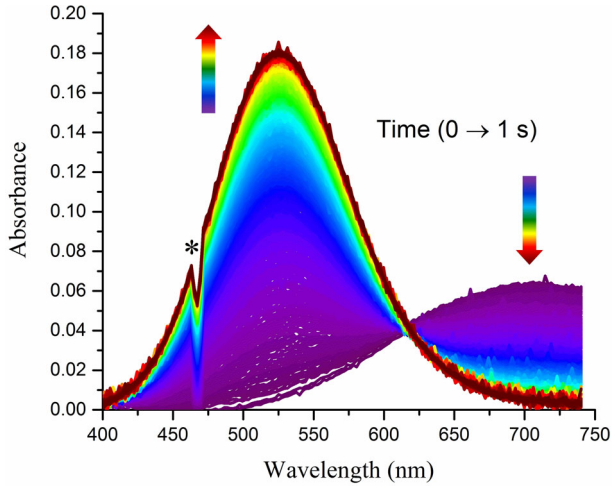

Figure 1. Typical diode-array stopped-flow experiment for 2 mM GGH peptide and 1.6 mM $CuCl_2$ (final concentrations). *Spectrophotometer lamp artefact.

was identical to that of the 4N complex of GGH published recently,[21] was completed within 1 s.

The 705 nm band at the start of the experiment, which was observed instead of the expected Cu^{2+} aqua ion band, $\lambda_{max} =$ 816 nm, (Figure S1 in the Supporting Information) provides direct evidence for the rapid formation within the dead time of the stopped-flow instrument of an intermediate Cu^{II} complex (IC), not reported previously. MES does not form Cu^{II} complexes[17,18] and is thus not responsible for the 705 nm band, as confirmed in Figure S1. The reference data for 1N, 2N, 3N, and 4N complexes of oligopeptides, collected in the Supporting Information Table S1, indicate that the 705 nm band could originate in a complex containing the Cu^{II} coordination to the $N_{im} + NH_2$ donor set. Otherwise the participation of a deprotonated peptide nitrogen (N^-) instead of either N_{im} or NH_2 would blueshift the *d–d* band to around 650 nm. The same result is obtained using the empirical equation derived by Sigel and Martin [Eq. (S1)].[22]

Further insight into the character of IC was obtained from the pH dependence of Cu^{II} binding to GGH provided by previously published potentiometric titrations.[21] The main 4N species present above pH 4 is described by stoichiometric formula $CuH_{-1}L$ and $CuH_{-2}L$, depending on the carboxyl protonation state ($pK_a = 4.68$). The negative hydrogen ion index denotes the Cu^{II}-assisted removal of Gly and His peptide nitrogen protons (see the Supporting Information Table S2 for the relationship between overall Cu^{II}/GGH complex stoichiometries and their coordination modes). The presence of partially coordinated Cu^{II}/GGH complexes in addition to the 4N complex has not been clarified by previous potentiometric studies,[19,20] but in a recent study the CuHL complex was identified at pH 3.5–5.0, and it was assigned to 2N coordination.[21] The protonation stoichiometry of this complex supports the macro-chelate structure involving the $N_{im} + NH_2$ donor set (see Table S2 for details).

The participation of a 2N complex in the coordination equilibrium was verified by performing the UV/Vis spectroscopic pH titration of Cu^{II}/GGH at the Cu^{II} concentration of 4.5 mM, five times higher than was used in the previous study.[21] A specific absorption band around 700 nm was now clearly observed at pH 4.2–4.7 (Figure 2A). This range is consistent with the species distribution calculated using the published data, which has the peak of the 2N form at pH 4.3 (Figure S3A).[21] Next, the UV/Vis spectra were recorded at pH 4.5 for increasing concentrations of Cu^{II}/GGH (Figure 2B). The obtained concentration dependence of a complex absorbing around 700 nm was in agreement with potentiometric results (Figure S3B), thus verifying the participation of a 2N complex analogous to IC at equilibrium in weakly acidic solutions. The apparent *d–d* band redshift at lower concentrations was due to its overlap with the Cu^{2+} aqua ion band at 816 nm (compare Figure S1 and Figure S3A).

Although the timescale for the 2N IC was determined directly, its formation from the Cu^{2+} aqua ion occurred within the 2 ms dead time of stopped-flow experiments. In order to gain qualitative insight into the early phase of reaction we resorted to the MHQ technique. The reactions, performed using the final concentrations of 2.0 mM GGH and 1.6 mM

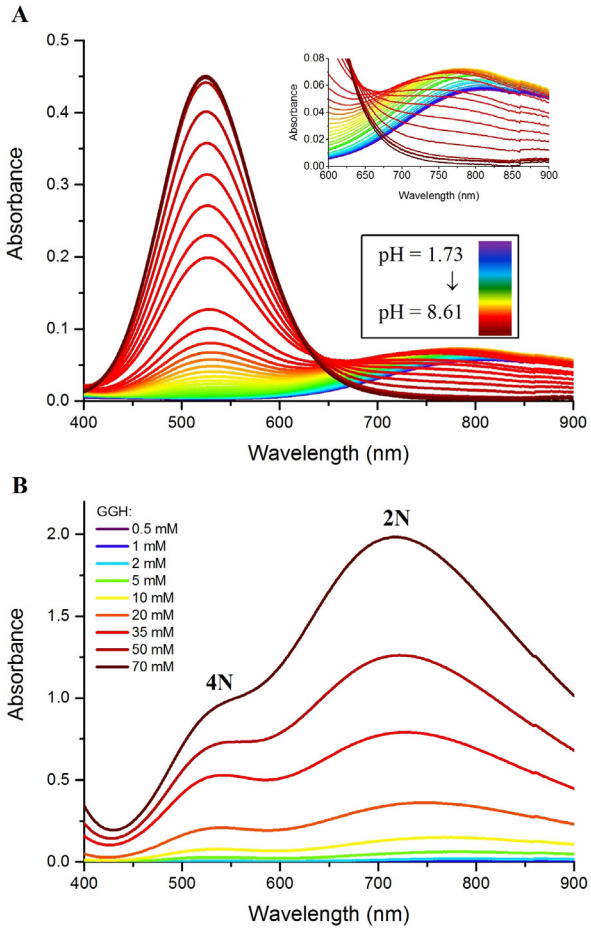

Figure 2. A) UV/Vis pH-metric titration of 5 mM GGH in the presence of 4.5 mM $CuCl_2$; the spectra are rainbow-coded from purple (pH 1.73) to red (pH 8.61). The inset expands the 600 to 900 nm range. B) Concentration dependence of the UV/Vis spectra of Cu^{II}/GGH complexes at pH 4.5. The GGH concentrations are given on the plot, the GGH/Cu^{II} ratio was 1:0.9.

Cu^{II}, were quenched at different reaction times between 100 μs and 1 s, (including freezing time) followed by the determination of the composition of rapidly frozen samples by EPR spectroscopy. The selected spectra are presented in Figure 3 (all spectra are given in Figure S7) Four different Cu^{II} species were readily detected, the Cu^{2+} aqua ion at the beginning of the reaction and up to 800 μs, and three different peptide-bound species. The first, early complex (EC) was present already at 100 and 200 μs and had disappeared by 2 ms; the second transient Cu^{II} complex species (IC) was best seen at 2 ms; the third, appearing first at 50 ms was fully dominant at 1 s. The EPR spectral parameters of these complexes are provided in Table S3. The latter two species can be readily identified as 2N and 4N complexes observed by stopped-flow, respectively, with full agreement of their times of appearance, and further confirmed by control EPR spectra of equilibrium samples at pH 4.5 and 6.0 (Figure S8). The EC can be tentatively assigned a 1N coordination based on its parameters. The course of the reaction is given in Scheme 1.

To verify this model, we performed further stopped-flow experiments at pH 6.0, varying the Cu^{II}/GGH ratio from 0.3 to 0.9. The obtained time-resolved spectra were analyzed using singular value decomposition (SVD). The formation of the 4N complex from IC was observed between 2 ms and 1 s,

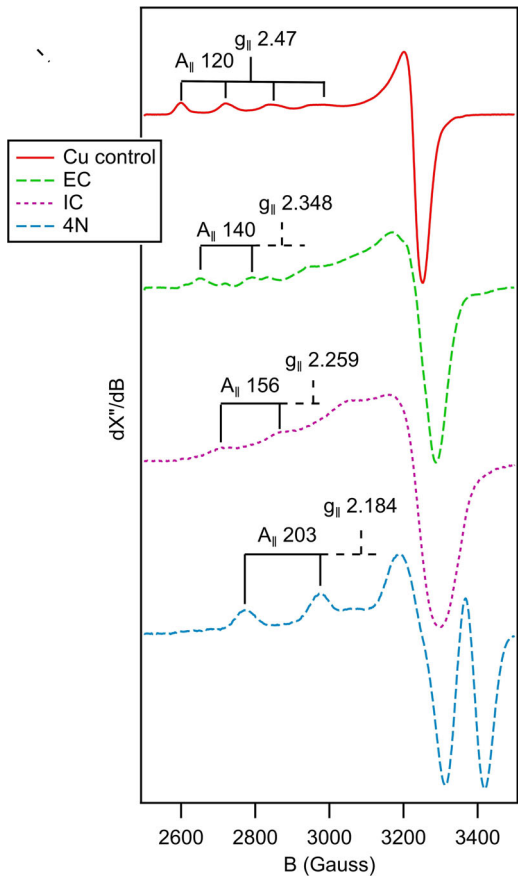

Figure 3. Representative spectra of the different species observed during the MHQ experiment, normalized for maximal signal amplitude. EPR conditions: microwave frequency, 9.405 GHz; 2 mW; modulation frequency, 100 kHz; modulation amplitude, 2.0 mT; temperature, 40 K.

$$\mathrm{GGH} + \mathrm{Cu}^{2+} \underset{k_{off1}}{\overset{k_{on1}}{\rightleftharpoons}} \mathrm{Cu(GGH)_{EC}} \underset{k_{off2}}{\overset{k_{on2}}{\rightleftharpoons}} \mathrm{Cu(GGH)_{IC}} \underset{k_{off3}}{\overset{k_{on3}}{\rightleftharpoons}} \mathrm{Cu(GGH)_{4N}}$$

Scheme 1. The proposed mechanism of Cu^{II} reaction with GGH yielding the 4N complex and definitions of accompanying rate constants.

with $k_{on3} = 6.674 \pm 0.003\ s^{-1}$ for the Cu^{II}/GGH ratio of 0.9, increasing linearly by circa $2\ s^{-1}$ up to the ratio of 0.3 (Figure S2B). To find the reason for this dependence on the Cu^{II} concentration, we carefully investigated the obtained spectra. The molar fraction of Cu^{II} bound in 2N species at the beginning of observation was less than 1 (Figure S4) in the whole Cu^{II} concentration range, as determined from spectral intensities at 705 nm. This finding contributes to the explanation of the observed reaction slowdown at low GGH excess. The reaction endpoint was the complete formation of the 4N complex, in accordance with the equilibrium experiments (Figure S3). Therefore, some Cu^{II}/EC, present at the beginning of observation, ought to form the IC and then 4N during the observation period. The overall reaction of IC formation includes the 2nd order step, which is the EC formation. It will be thus accelerated by GGH excess, as observed through the 4N complex formation rate.

The value of k_{off3} could not be determined from kinetic experiments, but instead, it can be estimated from the equilibrium condition at pH 6, in which the concentration ratio of 4N to 2N complexes ($[CuH_{-1}L] + [CuH_{-2}L]$)/[CuHL] is circa 2600 (see Figure S3A). This yields the k_{off3} value of $2.6 \times 10^{-3}\ s^{-1}$ for the Cu^{II}/GGH ratio of 0.9. The reconstructed spectra of individual complexes obtained from the SVD analysis agree well with the spectra of 2N and 4N complexes obtained directly at the beginning and the end of reaction with the maxima at 703 ± 2 nm and 527 ± 2 nm, respectively (see Figure S2A).

As discussed above, both the IC observed transiently at pH 6.0 and the CuHL complex contributing to equilibrium at lower pH values have the (N_{im} + NH_2) 2N coordination. These two groups can, however, be arranged around the Cu^{II} ion in two general configurations, 2 N-*cis* and 2 N-*trans*. A *cis/trans* equilibrium was demonstrated in temperature-dependent studies of the 2N $Cu(Gly)_2$ complex.[24] In the discussed complex two *cis* conformers are possible, with the peptide chain around or away from the Cu^{II} (2 N-*cis(endo)* and *cis(exo)* in Scheme 2). All three proposed 2N isomers should be easily formed from the EC (assumed to be 1N), but only the 2 N-*cis(endo)* conformer appears to be sterically suited for the concerted attack of the Cu^{II} ion on the peptide nitrogens, to yield the thermodynamically stable 4N complex. Other conformers can also be formed, for example, involving a Cu^{II}–N_{π} bond.

As a proof of concept for the *cis/trans* equilibrium we investigated the temperature dependence of absorption spectra for 20 mM GGH and 18 mM Cu^{II} at pH 4.5 (Figure S6). Between 5 °C and 45 °C, we observed the increase of intensity of the 4N complex, present as a minor species, probably due to a shift of 2N/4N equilibrium. More importantly, however, the other band, initially at 743 nm at 5 °C increased and redshifted systematically by up to circa 8 nm at 45 °C. A

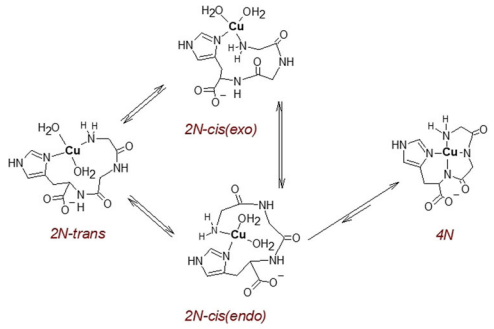

Scheme 2. Proposed structures of three putative 2N Cu(GGH) isomers and the pathway towards the 4N Cu(GGH) complex.

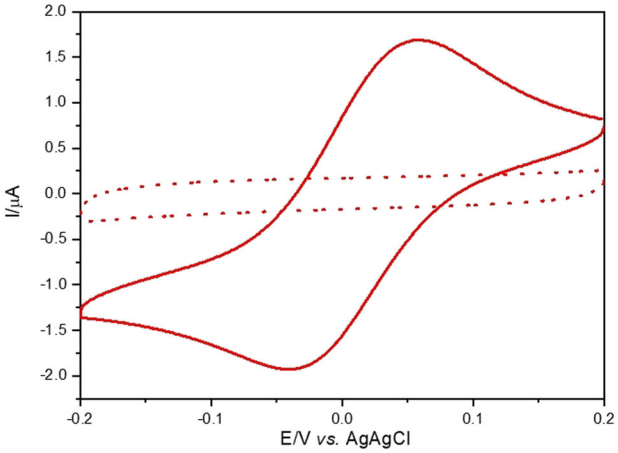

Figure 4. Solid line: the Cu^{I}/Cu^{II} electrochemical couple generated by the 2N Cu^{II}(GGH) complex, recorded for 0.45 mM Cu^{II}, 1 mM GGH, in 100 mM KNO_3/HNO_3, pH 5.0. Dashed line: 1 mM GGH alone under the same conditions.

simple shift of Cu^{2+}/2N equilibrium would cause either a band increase and blueshift (more 2N) or a band decrease and redshift (more free Cu^{2+}). Hence, the band increase and redshift was likely caused by a change of the 2N chromophore akin to that observed in $Cu(Gly)_2$, indicating a *cis/trans* equilibrium in the 2N Cu(GGH) complex.

The nitrogen ligand rearrangements between the hypothetical 2N species proposed in Scheme 2 require breaking and re-forming of Cu–N bonds, posing high activation energy barriers between them. The 2 N-*cis(endo)* conformer yielding the 4N complex is particularly sterically crowded, and hence likely to be the least stable, least populated local minimum in the energy landscape for Cu^{II} binding to GGH. We propose that this feature is responsible for the kinetic stability of IC.

Further evidence for the above mechanism can be obtained from preliminary stopped-flow experiments ran at higher pH values. The kinetic traces at 525 and 704 nm obtained in HEPES at pH 7.0, 7.4 and 8.0 are compared with the reaction at pH 6.0 in MES in Figure S5. The rearrangement of 2N IC into 4N is only slightly accelerated with the increased pH. In the only previous study of dissociation kinetics of Cu^{II}/GGH, the formation of a hypothetical 3N rather than 2N species was proposed as rate-limiting, with the protonation of the amide nitrogen as key event.[25] We have directly identified the conversion of the 2N to 4N complex as rate limiting. The data in Figure S5 show that the protonation of amide nitrogen atoms has only a secondary contribution to the observed rates because the 2N complex decay and 4N complex formation rates increase merely about two-fold vs. the 100-fold $[H^+]$ decrease over the tested pH range. This observation is compatible with the rearrangement of the 2N species as rate limiting, as this process (Scheme 2) has no net proton dependence. Otherwise, a very strong quadratic rate dependence on pH would be expected.

Figure 4 presents a cyclic voltammogram (CV) for Cu^{II}/GGH recorded at pH 5, exhibiting a quasi-reversible Cu^{I}/Cu^{II} redox couple with the reduction peak at -0.034 ± 0.003 V and the oxidation peak at 0.056 ± 0.002 V. The 2N form of Cu^{II}/GGH could be electrochemically determined only in a carefully selected range of potentials and under excess of peptide over Cu^{II} ions. This is due to the fact that even a small amount of non-complexed Cu^{2+} ions present in solution strongly interferes with the electrochemical response of Cu^{II}/GGH complexes, by generating a typical adsorption peak of two-electron Cu^{2+} reduction and Cu^0 deposition on the electrode surface (Figure S9). The Cu^{I}/Cu^{II} redox couple was not identified on a CV curve registered at pH 7.4, while sweeping the potential in the negative direction (from the initial value, $E_{in} = 0.5$ V). As expected, an irreversible oxidation peak attributed to a reactive Cu^{III} species was detected at 0.774 ± 0.004 V (pH 5.0) and 0.798 ± 0.002 V (pH 7.4) (Figure S10).[7,12,26] The irreversibility of the Cu^{II}/Cu^{III} redox process can be explained by rapid oxygen-induced decarboxylation followed by hydroxylation at the carboxyl end of Cu^{II}-complexed GGH, occuring via a Cu^{III} intermediate.[27] The electrochemical behavior of Cu^{II}/GGH at pH 7.4 confirms the predominance of the 4N complex indicated by equilibrium species distribution.

The electrochemical competence of the 2N complex is in a perfect match with the recent mass spectrometry study which proposed the $N_{im} + NH_2$ coordination for the Cu^{I} ion bound to the ATCUN/NTS motif.[28] DFT calculations indicated the 2N-*trans* structure for the Cu^{I} complex. Therefore, it is plausible to suggest that the temperature-dependent *cis/trans* equilibration in the Cu^{II} complex might be responsible for the observed properties of the electrochemical process. A similar phenomenon was recently demonstrated for the ROS generating Cu^{I}/Cu^{II} redox couple of Alzheimer's $A\beta_{1\text{-}16}$ model peptide.[29] Indeed, the detection of the Cu^{I}/Cu^{II} redox activity in the GGH complex explains the recently reported inhibition of slow ascorbate-induced ROS production by 4N Cu^{II} complexes of DAHK, KGHK, and FRHD-NH_2 peptides specifically by Cu^{I} chelators.[13] More generally, it explains how some ATCUN/NTS complexes are redox active towards mild electron donors/acceptors, such as ascorbate/H_2O_2, despite the electrochemical studies reporting only the (often irreversible) Cu^{II}/Cu^{III} process at potentials around 0.8 V vs. Ag/AgCl, possibly too high to be physiologically relevant.[12,26] The ROS generation may be enabled by even minute amounts of the redox-active complex still present at physiological pH, as reported for example, for Cu^{2+} aqua ion.[30] Therefore, the relative abundance of the 2N

and 4N species under given conditions emerges as key factor in the redox activity of ATCUN/NTS complexes.

The discovery of a long-lived 2N kinetic intermediate (IC) in the interaction of Cu^{II} ions with GGH, a prototypical ATCUN/NTS motif, together with the demonstration of its ability to maintain the redox activity of copper, is a game-changer in the understanding of the ATCUN/NTS reactivity, and further, of molecular mechanisms of biological copper transport. The time scale of hundreds of milliseconds is sufficient for 2N complexes to engage in interactions with other partners, such as receptors, membrane transporters, enzymes, carrier proteins, and small molecules. This study paves way to studies of kinetic and redox properties of ATCUN/NTS motifs of HSA and hCtr1, aimed at explaining the mechanism of copper delivery to cells.

Acknowledgements

This research was financed by National Science Centre of Poland (NCN) grants no. 2018/29/B/ST4/01634 to W.B. and 2018/31/N/ST5/02556 to R.K. and by Warsaw University of Technology statutory funds. The equipment used at IBB PAS was sponsored, in part, by the Centre for Preclinical Research and Technology (CePT), a project co-sponsored by the European Regional Development Fund and Innovative Economy, The National Cohesion Strategy of Poland. PLH acknowledges financial support from grant NWO-CW 711.014.006 from the Council for Chemical Sciences of The Netherlands Organization for Scientific Research.

Conflict of interest

The authors declare no conflict of interest.

Keywords: amino-terminal copper and nickel (ATCUN) motif · copper · electrochemistry · EPR spectroscopy · peptides

[1] a) R. Squitti, *J. Trace Elem. Med. Biol.* **2014**, *28*, 482; b) J. Lowe, R. Taveira-da-Silva, E. Hilário-Souza, *IUBMB Life* **2017**, *69*, 255; c) A. G. Ranjbary, M. Mehrzad, H. Dehghani, A. Abdollahi, S. Hosseinkhani, *Biol. Trace Elem. Res.* **2020**, *194*, 66.
[2] a) N. Camerman, A. Camerman, B. Sarkar, *Can. J. Chem.* **1976**, *54*, 1309; b) W. Bal, M. I. Djuran, D. W. Margerum, E. T. Gray, M. A. Mazid, R. T. Tom, E. Nieboer, P. J. Sadler, *J. Chem. Soc. Chem. Commun.* **1994**, *113*, 1889; c) S. L. Best, T. K. Chattopadhyay, M. I. Djuran, R. A. Palmer, P. J. Sadler, I. Sóvágó, K. Varnagy, *J. Chem. Soc. Dalton Trans.* **1997**, 2587.
[3] C. Hureau, H. Eury, R. Guillot, C. Bijani, S. Sayen, P.-L. Solari, E. Guillon, P. Faller, P. Dorlet, *Chem. Eur. J.* **2011**, *17*, 10151.
[4] V. A. Streltsov, R. S. K. Ekanayake, S. C. Drew, C. T. Chantler, S. P. Best, *Inorg. Chem.* **2018**, *57*, 11422.
[5] E. Stefaniak, D. Płonka, S. C. Drew, K. Bossak-Ahmad, K. L. Haas, M. J. Pushie, P. Faller, N. E. Wezynfeld, W. Bal, *Metallomics* **2018**, *10*, 1723.
[6] W. Bal, G. N. Chmurny, B. D. Hilton, P. J. Sadler, A. Tucker, *J. Am. Chem. Soc.* **1996**, *118*, 4727.
[7] P. Gonzalez, K. Bossak, E. Stefaniak, C. Hureau, L. Raibaut, W. Bal, P. Faller, *Chem. Eur. J.* **2018**, *24*, 8029.
[8] a) T. Peters in *Advances in Protein Chemistry*, Elsevier, **1985**, pp. 161 – 245; b) W. Bal, M. Sokołowska, E. Kurowska, P. Faller, *Biochim. Biophys. Acta Gen. Subj.* **2013**, *1830*, 5444.
[9] K. L. Haas, A. B. Putterman, D. R. White, D. J. Thiele, K. J. Franz, *J. Am. Chem. Soc.* **2011**, *133*, 4427.
[10] A. Santoro, N. E. Wezynfeld, E. Stefaniak, A. Pomorski, D. Płonka, A. Krężel, W. Bal, P. Faller, *Chem. Commun.* **2018**, *54*, 12634.
[11] E. Stefaniak, W. Bal, *Inorg. Chem.* **2019**, *58*, 13561.
[12] M. Z. Wiloch, U. E. Wawrzyniak, I. Ufnalska, A. Bonna, W. Bal, S. C. Drew, W. Wróblewski, *J. Electrochem. Soc.* **2016**, *163*, G196 – G199.
[13] A. Santoro, G. Walke, B. Vileno, P. P. Kulkarni, L. Raibaut, P. Faller, *Chem. Commun.* **2018**, *54*, 11945.
[14] a) M. D. J. Libardo, S. Nagella, A. Lugo, S. Pierce, A. M. Angeles-Boza, *Biochem. Biophys. Res. Commun.* **2015**, *456*, 446; b) M. D. J. Libardo, V. Y. Gorbatyuk, A. M. Angeles-Boza, *ACS Infect. Dis.* **2016**, *2*, 71; c) M. D. J. Libardo, A. A. Bahar, B. Ma, R. Fu, L. E. McCormick, J. Zhao, S. A. McCallum, R. Nussinov, D. Ren, A. M. Angeles-Boza, et al., *FEBS J.* **2017**, *284*, 3662.
[15] a) T. T. K. Nguyen, H. V. Tran, T. T. Vu, S. Reisberg, V. Noël, G. Mattana, M. C. Pham, B. Piro, *Biosens. Bioelectron.* **2019**, *127*, 118; b) O. Synhaivska, Y. Mermoud, M. Baghernejad, I. Alshanski, M. Hurevich, S. Yitzchaik, M. Wipf, M. Calame, *Sensors* **2019**, *19*, 4022.
[16] a) F. G. M. Wiertz, O.-M. H. Richter, A. V. Cherepanov, F. MacMillan, B. Ludwig, S. de Vries, *FEBS Lett.* **2004**, *575*, 127; b) B. Srour, M. J. F. Strampraad, W. R. Hagen, P.-L. Hagedoorn, *J. Inorg. Biochem.* **2018**, *184*, 42.
[17] H. E. Mash, Y.-P. Chin, L. Sigg, R. Hari, H. Xue, *Anal. Chem.* **2003**, *75*, 671.
[18] N. E. Good, G. D. Winget, W. Winter, T. N. Connolly, S. Izawa, R. M. Singh, *Biochemistry* **1966**, *5*, 467.
[19] R. W. Hay, M. M. Hassan, C. You-Quan, *J. Inorg. Biochem.* **1993**, *52*, 17.
[20] E. Farkas, I. Sóvágó, T. Kiss, A. Gergely, *J. Chem. Soc. Dalton Trans.* **1984**, 611.
[21] K. Bossak-Ahmad, T. Frączyk, W. Bal, S. C. Drew, *ChemBioChem* **2020**, *21*, 331.
[22] H. Sigel, R. B. Martin, *Chem. Rev.* **1982**, *82*, 385.
[23] H. Kozłowski, W. Bal, M. Dyba, T. Kowalik-Jankowska, *Coord. Chem. Rev.* **1999**, *184*, 319.
[24] R. Biswas, M. Koley, *World J. Chem. Educ.* **2017**, *5*, 185.
[25] L. F. Wong, J. C. Cooper, D. W. Margerum, *J. Am. Chem. Soc.* **1976**, *98*, 7268.
[26] M. Mital, N. E. Wezynfeld, T. Frączyk, M. Z. Wiloch, U. E. Wawrzyniak, A. Bonna, C. Tumpach, K. J. Barnham, C. L. Haigh, W. Bal, et al., *Angew. Chem. Int. Ed.* **2015**, *54*, 10460; *Angew. Chem.* **2015**, *127*, 10606.
[27] P. de Meester, D. J. Hodgson, *Inorg. Chem.* **2002**, *41*, 440.
[28] S. Carlotto, A. Bonna, K. Bossak-Ahmad, W. Bal, M. Porchia, M. Casarin, F. Tisato, *Metallomics* **2019**, *11*, 1800.
[29] C. Cheignon, M. Jones, E. Atrián-Blasco, I. Kieffer, P. Faller, F. Collin, C. Hureau, *Chem. Sci.* **2017**, *8*, 5107.
[30] M. Mital, I. A. Zawisza, M. Z. Wiloch, U. E. Wawrzyniak, V. Kenche, W. Wróblewski, W. Bal, S. C. Drew, *Inorg. Chem.* **2016**, *55*, 7317.

Manuscript received: March 23, 2020
Accepted manuscript online: April 8, 2020
Version of record online: ■■ ■■, ■■■■

Communications

Bioinorganic Chemistry

R. Kotuniak, M. J. F. Strampraad, K. Bossak-Ahmad, U. E. Wawrzyniak, I. Ufnalska, P.-L. Hagedoorn, W. Bal* _____ ▮▮▮▮–▮▮▮▮

Key Intermediate Species Reveal the Copper(II)-Exchange Pathway in Biorelevant ATCUN/NTS Complexes

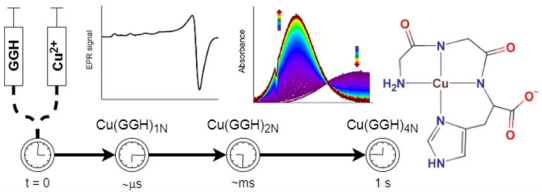

ATCUN/NTS motifs participate in physiological Cu^{II} exchange. Using kinetic methods, spectroscopy, and electrochemistry, it was demonstrated that Cu^{II} binding to GGH, an ATCUN/NTS representative, proceeds via partially coordinated species. The 2N-coordinated complex with $t_{1/2} \approx 100$ ms (pH 6.0) and Cu^{II}/Cu^{I} redox activity is the long-sought reactive intermediate for extracellular copper delivery.

